

The 2014 Earthquake in Iquique, Chile: Comparison between Local Soil Conditions and Observed Damage in the Cities of Iquique and Alto Hospicio

Alix Becerra,^{a)} Esteban Sáez,^{a),b)} Luis Podestá,^{a),b)} and Felipe Leyton^{c)}

In this study, we present comparisons between the local soil conditions and the observed damage for the 1 April 2014 Iquique earthquake. Four cases in which site effects may have played a predominant role are analyzed: (1) the ZOFRI area, with damage in numerous structures; (2) the port of Iquique, in which one pier suffered large displacements; (3) the Dunas I building complex, where soil-structure interaction may have caused important structural damage; and (4) the city of Alto Hospicio, disturbed by the effects of saline soils. Geophysical characterization of the soils was in agreement with the observed damage in the first three cases, while in Alto Hospicio the earthquake damage cannot be directly related to geophysical characterization. [DOI: 10.1193/111014EQS188M]

INTRODUCTION

On 1 April 2014, a M_W 8.2 earthquake occurred in northern Chile, northwest of the town of Iquique; the main shock was followed by a M_W 7.7 aftershock two days later (Figure 1). The 2014 Iquique earthquake was caused by the thrust faulting between the Nazca and South America plates. The rupture area had a length of about 200 km and a hypocenter depth of 38.9 km, according to the Chilean Seismological Center earthquake report. Prior to this event, northern Chile was characterized by a seismic quiescence of 136 years (known as the “Iquique seismic gap”; Comte and Pardo 1991). Historical records indicate a M8.8 earthquake in 1877, and since then, a cumulative seismic moment deficit of $17.2 \times 10e + 21$ Nm had been registered up to 2011 (Chlieh et al. 2011). This scenario suggested that a major event was imminent.

The purpose of this research is to perform a preliminary assessment of the observed damage in the city of Iquique produced by the 2014 Iquique earthquake and to evaluate the potential contribution of site effects to damage patterns. The first section describes some of the available strong motion records. The sections of this article, from *Background* through *Damage Observations*, present a detailed study of the damage reconnaissance campaign after the earthquake and describe four case studies that were particularly interesting for

^{a)} Department of Geotechnical and Structural Engineering, Pontificia Universidad Católica de Chile, Vicuña Mackenna 4860, Macul, Santiago, Chile. 7820436. esaez@ing.puc.cl

^{b)} Center for Integrated Natural Disaster Management CONICYT/FONDAP/15110017, Vicuña Mackenna 4860, Macul, Santiago, Chile. 7820436

^{c)} National Seismological Center, University of Chile, Beauchef 850, Santiago, Chile. 8370448

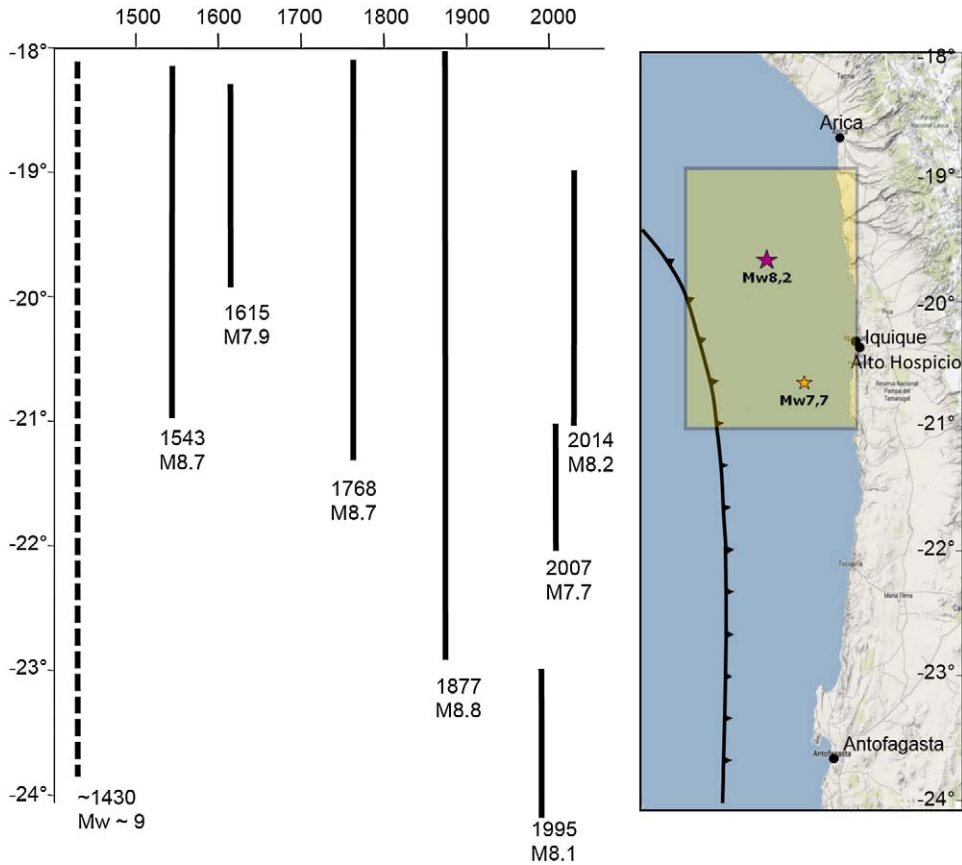


Figure 1. Historical record of great earthquakes in northern Chile (modified from Comte and Pardo 1991) and rupture zone of the 2014 Iquique earthquake. The marked square indicates the estimated area of rupture according to the USGS earthquake report (USGS 2014).

this comparison: (1) the ZOFRI industrial zone; (2) the port of Iquique; (3) the Dunas I building complex; and (4) the city of Alto Hospicio, which is adjacent to Iquique. Each case study is described and compared to a geophysical characterization of the subsurface. The final section presents the conclusions of the study.

BACKGROUND

Iquique and Alto Hospicio are two adjacent cities located in northern Chile, west of the Coastal Range escarpment (Figure 1). Among the main urban areas in the north of the country, these two represent the ones most affected by the 2014 Iquique earthquake. In this regard, we focused on damage evaluation and the potential contribution of site effects to the observed damage. Although no official statistics have been yet published regarding the damage caused by the earthquake, we observed that the major part of the damage is concentrated in low-height masonry structures (houses and warehouses of up to four stories).

SEISMIC INTENSITY IN IQUIQUE

The seismic intensity in Iquique can be characterized by traditional methodologies such as shakemaps that provide strong-motion indicators based on its distance to the epicenter and topography. Based on the shakemap available from the USGS (2014), an intensity of VI to VII, peak accelerations in the range of 0.12 g to 0.22 g, and peak velocities from 9.6 cm/s to 20 cm/s were estimated for the Iquique area. Nevertheless, Stations T03A and T08A of Figure 2 show higher accelerations and velocities than the available shakemap.

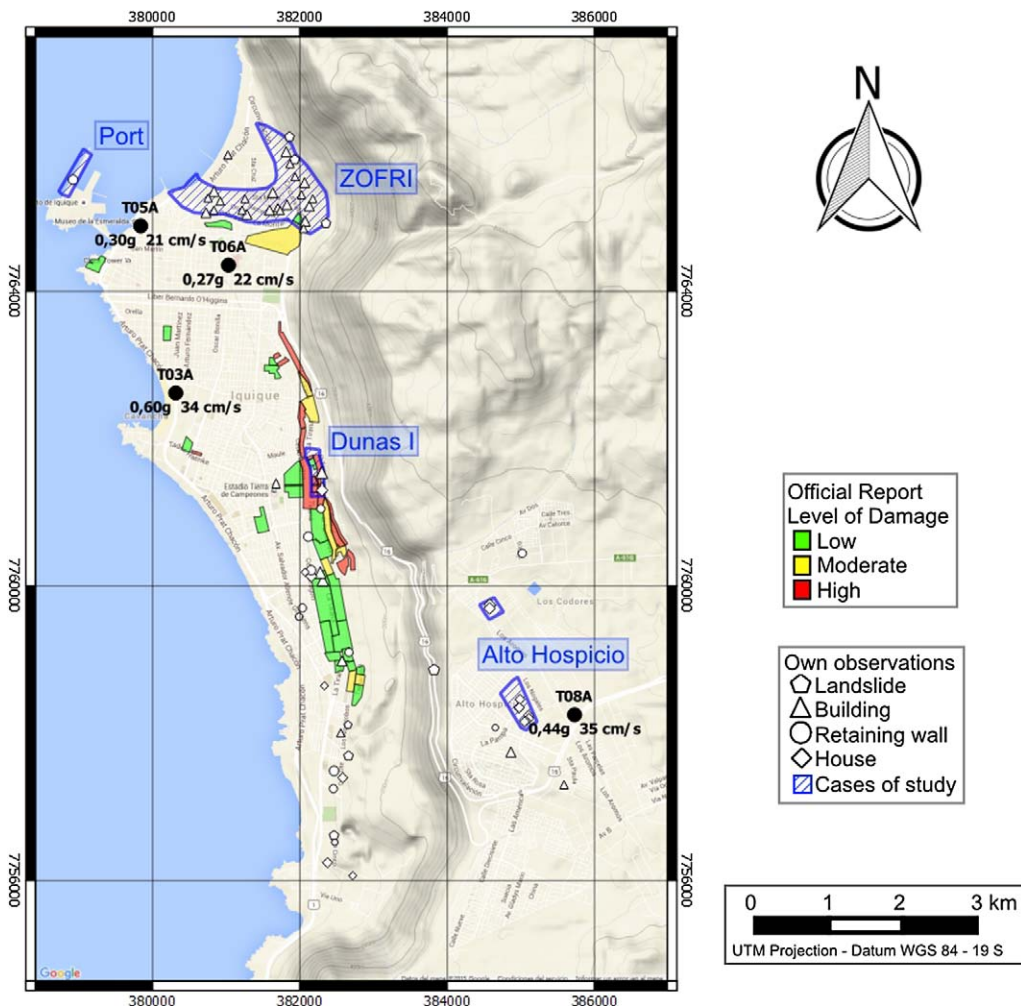


Figure 2. Observed damage in Iquique after the 2014 Iquique earthquake. Comparison between the official government report of damage (obtained from the Ministry of Housing and Urban Development) The size of the symbols represents, qualitatively, the level of damage observed in each case. Coordinates are in UTM, Datum WGS84. The figure also displays the seismic stations in Iquique and Alto Hospicio with their registered PGAs and PGVs.

It is worth noting that shakemaps are very simple models and may not be reliable at small scales. Indeed, shakemaps are typically enhanced with instrumental recordings, but because ground motions records from Iquique were not available to enhance this shakemap, PGAs and PGVs come from the very approximate correlations of intensity with these ground motion parameters, which could justify the observed differences with the local stations in Iquique. This, as well as the differential damage registered in the city after the earthquake, suggests that detailed studies are necessary to evaluate the site conditions in which the damage was observed.

There are several factors that affect the intensity of an earthquake; the distance to the ruptured fault is the most common one to develop ground motion attenuation relations. Nonetheless, there is a number of other variables that also must be considered, such as the type of buildings and local soil conditions. Geophysical studies were performed prior to the earthquake that provided a S-wave velocity and predominant period characterization along the soils of Iquique and Alto Hospicio (Becerra et al. 2014). This material will be valuable to assess the observed damage around both cities in the following sections.

STRONG MOTION RECORDS

The 2014 Iquique earthquake was registered by four seismic stations in the cities of interest. The location of each station is depicted in Figure 2. Additionally, the recorded peak ground accelerations (PGA) and peak ground velocities (PGV) are shown in the same figure. Several authors have established that PGA is well correlated with damage of short period structures, while PGV is well correlated with long period structures (e.g., Matsumura 1992), so both parameters may be useful to assess the seismic hazard along the city.

The differences in Iquique and Alto Hospicio are significant. In terms of accelerations, station T03A shows a PGA twice as large as station T05A (Figure 2), with a distance of barely 2 kilometers between them. In terms of Peak Ground Velocities there are some differences among the stations though they are not as significant as the former, with a maximum PGV of 35 cm/s in Alto Hospicio (station T08A).

Furthermore, a comparison between the strong motion records, the pseudo-acceleration response spectra and horizontal-to-vertical spectral ratios (HVSR) results are shown in Figure 3. The HVSR were obtained using microtremors a year before the earthquake (Becerra et al. 2015). In the cases of stations T05A and T06A, their spectra are characterized for their wide shape and low amplitude (less than 1.5). It is worth to mention that stations T03A, T05A, and T06A are located at sea level, while T08A is on the Coastal Range escarpment, a cliff with an altitude of about 550 m above sea level.

The pseudo-acceleration response spectra of (a) and (d) show a peak period of 0.16 s (6.25 Hz) and 0.08 s (12.5 Hz) for stations T03A and T08A, respectively; there are no noticeable differences between orientations for each spectra. Note that the peak period in T03A is twice as much as in the T08A station.

Additionally, Figure 3 displays the predominant frequency obtained on each station through HVSR or Nakamura's technique (Nakamura, 1989) using microtremor records a year before the earthquake. Solid lines indicate the mean ratios through all the analysis windows, while dashed lines correspond to one standard deviation from the mean.

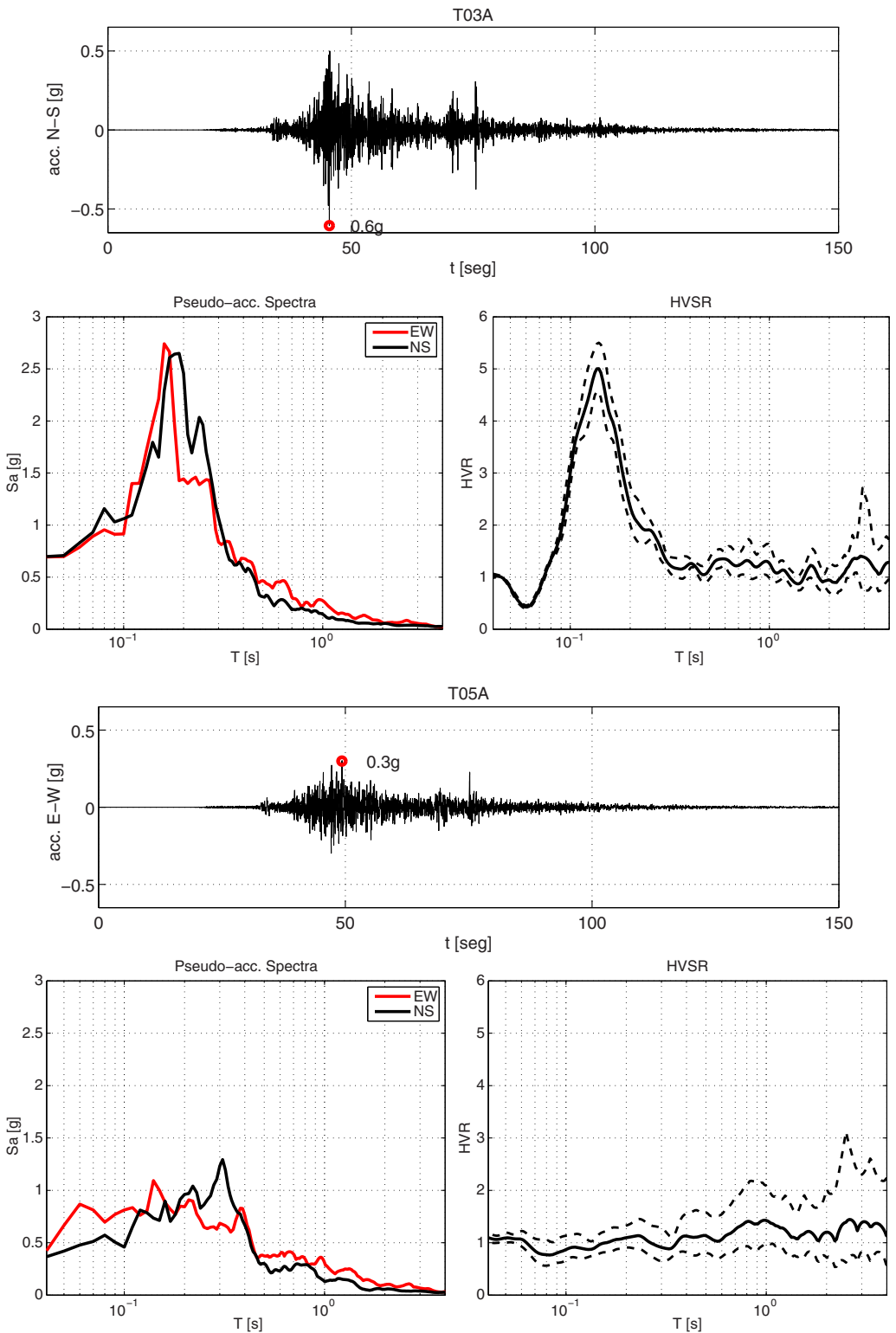


Figure 3. Strong motion records, pseudo-acceleration response spectra (5% damping) and HVSR results for the seismic stations located in Iquique and Alto Hospicio.

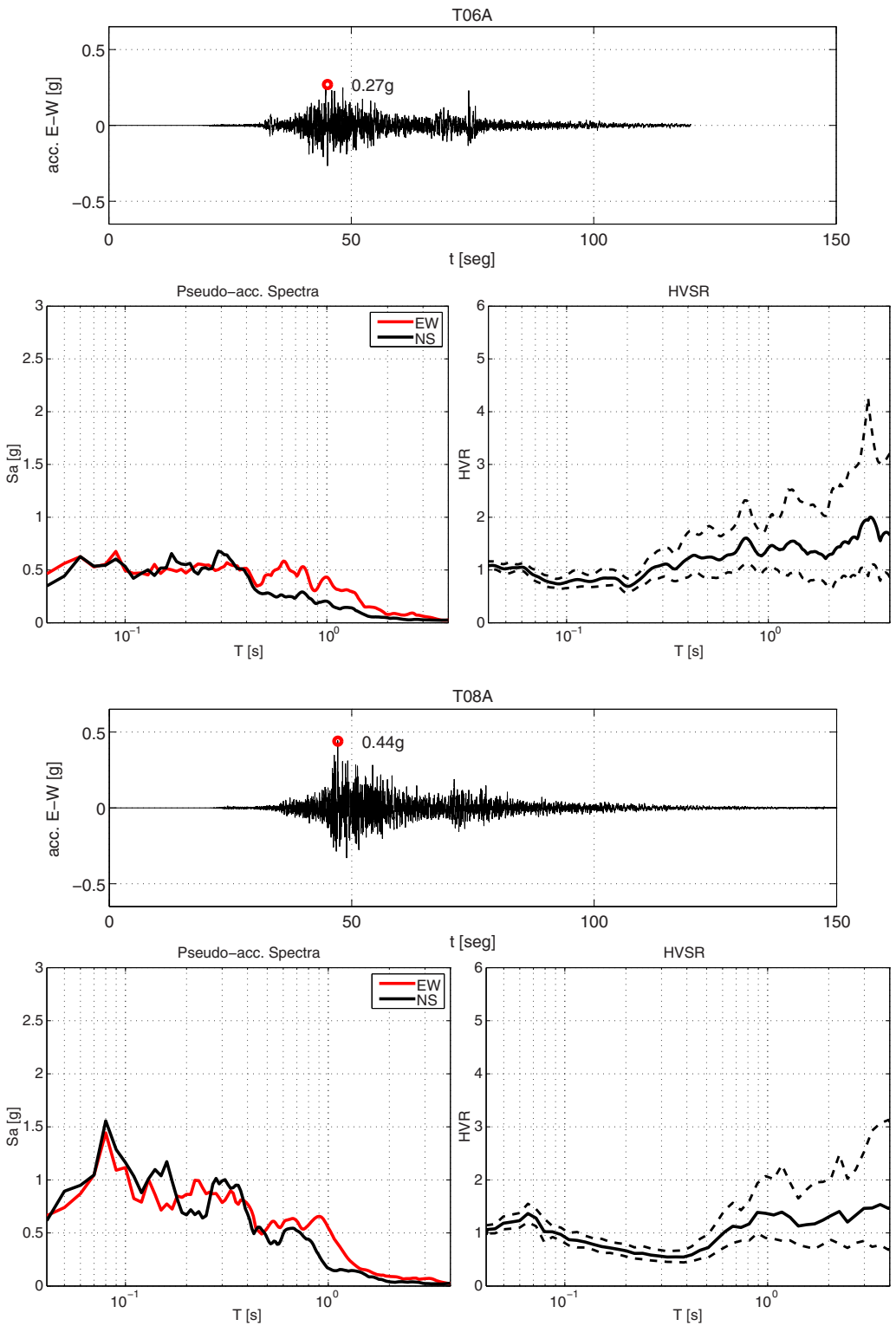


Figure 3. Continued.

The predominant frequency of the sites that show a clear peak, such as T03A, are in agreement with the shape of spectra of the strong motion records, particularly in the station that showed the highest PGA.

Although the peak in T08A is not clear in terms of SESAME (Acerra et al. 2004) criteria, it is rather similar to the results from the response spectra. The other two stations (T05A and T06A) do not show any clear peak in pseudo-acceleration response spectra or H/V spectral ratios, possibly due to the stiff soils characterizing the zone (Becerra et al. 2015).

DAMAGE OBSERVATIONS

The damage reconnaissance campaign took place in Iquique and Alto Hospicio between 9 and 13 April 2014, a week after the earthquake. During that period, we explored the entire cities and registered the zones where significant damage was concentrated. Figure 2 shows the observed damage in each city and marks the case studies that will be detailed in this research, it also shows the official government report of the registered damage in the city. In this figure, we may note that most of the damage observed in our reconnaissance campaign was observed in the north on the city. Very few cases were reported toward the southwest. In the south of the city, damage concentrates to the east and an unexpected high number of cases were detected in Alto Hospicio area. It is worth mentioning that in the center of the city, near stations T05A and T06A of Figure 2, no damage was observed, historical buildings of over a hundred years old remained intact, just as most of the other structures in the zone.

Generally, most of the houses and buildings within the cities did not undergo significant structural damage. To the southwest of the city, most of the damage was observed in collapsed retaining walls of low height (about 2 m) and masonry houses with shear wall failures. To the north, the area around the ZOFRI industrial zone was mostly affected, including some structural damage and fallen roof parapets of warehouses. In Alto Hospicio, structural damage was observed in some masonry houses of two stories along a well-defined zone.

In the following sections, we will detail four case studies within both cities, as shown in Figure 2. These cases are especially interesting, not because of the relationship between the different case studies, but rather because of the role that the ground amplification may have taken place in the types of damages observed.

CASE 1: ZOFRI

The ZOFRI is an industrial zone composed of mainly masonry warehouses which are confined structures of three to five levels. Most of this area is characterized by a moderate to thick layer of marine deposits. Toward the east, the thickness of this layer decreases (to about 20 m) and mixes with eolian deposits (Figure 4). This zone is enclosed by the coastal escarpment to the east of the city.

The observed damages in the zone are classified by type in Figure 5. Most of it is concentrated in fallen roof parapets, whereas little structural damage and few landslides were identified in the area. The relative soft soil layer and the topographic effects of the escarpment could increase accelerations in the zone, resulting in larger damage in structural and non-structural components, such as roof parapets (Figure 6b). Most parapets were built using

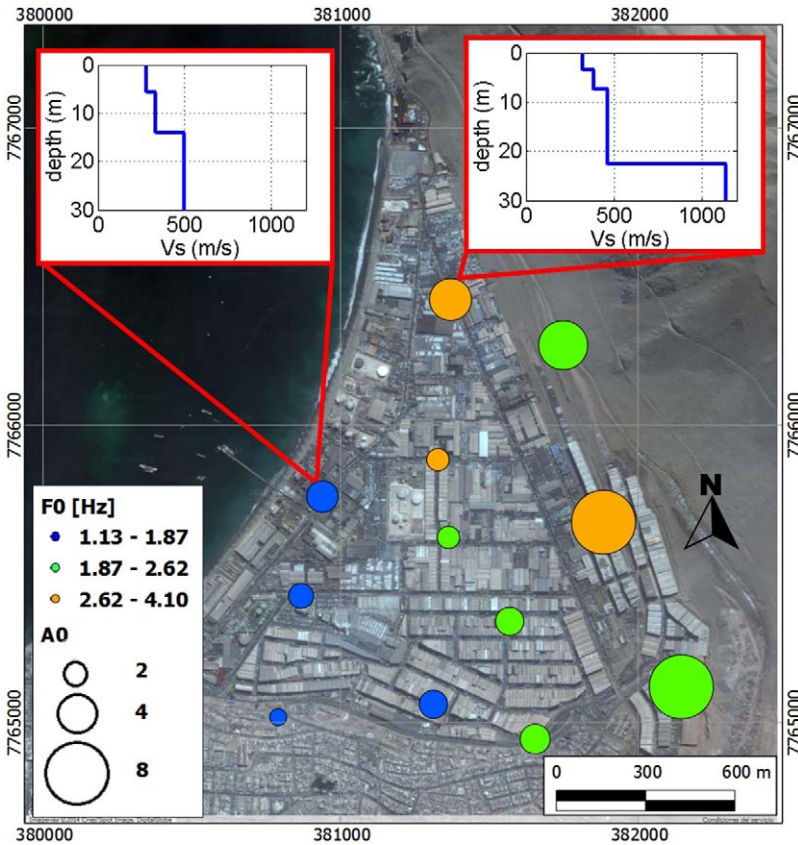


Figure 4. Geophysical characterization of the ZOFRI zone. The image shows the predominant frequency of the soil (obtained from HVSr using microtremors) and typical shear wave velocity profiles for two different areas (obtained by surface wave methods). The circle size represents the amplitude of the peak frequency while the color represents the frequency range.

concrete block with very little steel reinforcement and without any out-of-plane reinforcement; hence, they have extremely low resistance under transversal loading. Even if these elements could be considered as nonstructural, their failure is highly risky for people working in these warehouses. Indeed, the only fatality reported in ZOFRI was crushed by a falling parapet. As depicted in Figure 6a, most of the structural failures were located in short columns.

Figure 4 shows the predominant frequency of each site obtained through HVSr and typical shear wave velocity profiles for different zones; this figure also presents the corresponding amplitude of the HVSr. We can see that higher amplitudes characterize the data toward the east, which suggest a significant impedance contrast between the soil layers and the bedrock (Leyton et al. 2013). This result would strengthen the hypothesis of the increase in peak acceleration taking place in this area; however, we could not confirm this hypothesis because no seismographs were installed in this sector during the earthquake.

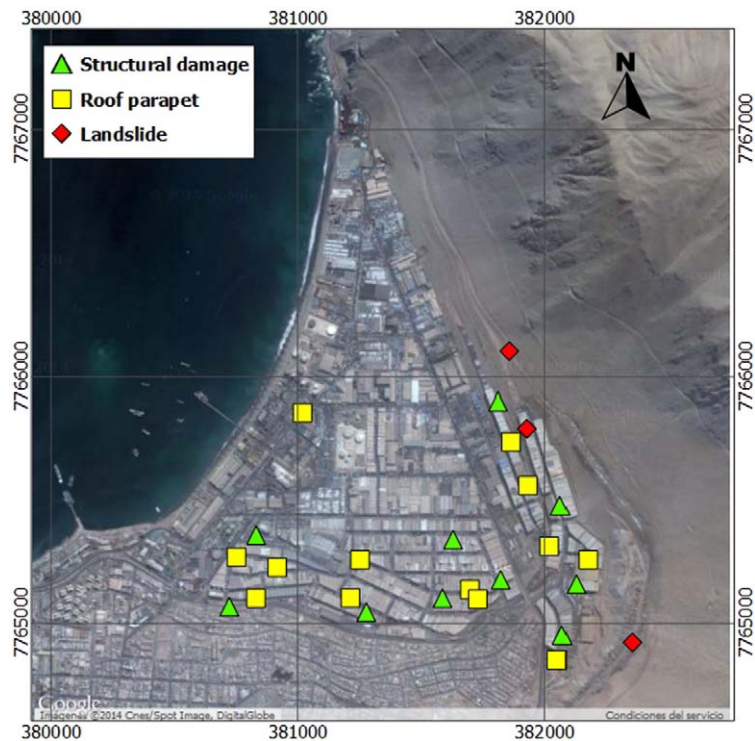


Figure 5. Classification of observed damage in the ZOFRI zone. Each symbol represents a type of damage, as shown in the upper left legend.

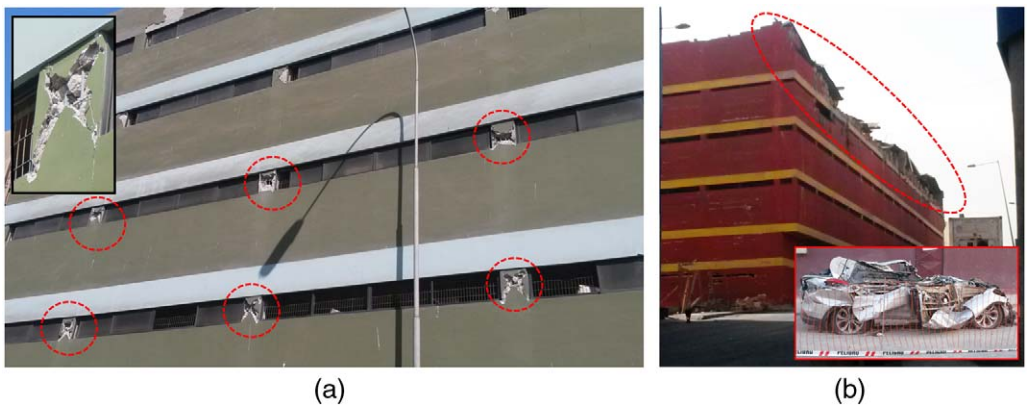


Figure 6. Examples of observed damage in the ZOFRI warehouses. (a) Short-column structural failure and (b) fallen roof parapet with the result of a crushed car.

The slopes located to the east of the ZOFRI zone have terraces to allow vehicle transit that were built using shallow compaction without any reinforcement or containment system; therefore, the landslides shown in Figure 5 were foreseeable. During the reconnaissance campaign, we measured a maximum horizontal displacement of 1.3 m by adding the opening of the cracks across straight lines parallel to the direction of sliding.

CASE 2: PORT OF IQUIQUE

The port of Iquique is located in the northwest part of the city (Figure 2). Previous studies classified the soil beneath the port into two types; the terminal and storage warehouses are built on bedrock, whereas the soil profile beneath the two piers consist of a deep layer of artificial landfill until reaching stiffer material Figure 8. The eastern pier was recently seismically reinforced, but the western pier has kept its original design from the 1920s. In order to estimate the depth of the artificial landfill, we assumed an average shear wave velocity of 300 m/s based on the geophysical surveys, and calculated the depth as

$$H = \frac{V_s}{4F_0} \quad (1)$$

Since the predominant frequency of the soil has been estimated in several points of the pier through the HVSr technique, it was possible to evaluate the change in thickness along the western pier, as shown in Figure 7. We can see that, in general, the thickness of the artificial landfill tends to increase toward the end of the pier, whereas toward the terminal it is thinner. Since a constant shear wave velocity is unlikely in sand deposits and artificial fills, this depth should be considered as an approximation only.

During the damage reconnaissance campaign, we observed that the terminal and eastern pier were practically intact after the earthquake. However, the western pier suffered large differential settlements all along its extension, especially toward the northeastern end, as shown in Figure 8.

The evidence during the reconnaissance campaign suggested that the cracks along the pier were caused by a horizontal displacement of the retaining lateral walls. Using a differential GPS, we measured the changes in elevation along three lines in the pier, as shown in Figure 9, where most of the variations are located to the right side, consistent with the fact that the retaining walls were higher on the left side of the figure. Hence, the variable height of the perimeter walls with a similar cross section could have induced this differentiated lateral displacement under the seismically increased lateral pressures from the fill. Furthermore, the variable thickness along the pier is consistent with the increased displacement toward the end of the pier. Given the poor compaction of the soil and the evidence during the reconnaissance campaign, some partial liquefaction could have taken place, as sand was vented through cracks in the surface of the pier (Rollins et al. 2014). Additionally, according to the Port's administration surveys, lateral spread is still taking place more than a month after the main shock. Detailed studies must be conducted to properly understand the complex mechanisms taking place in this case.

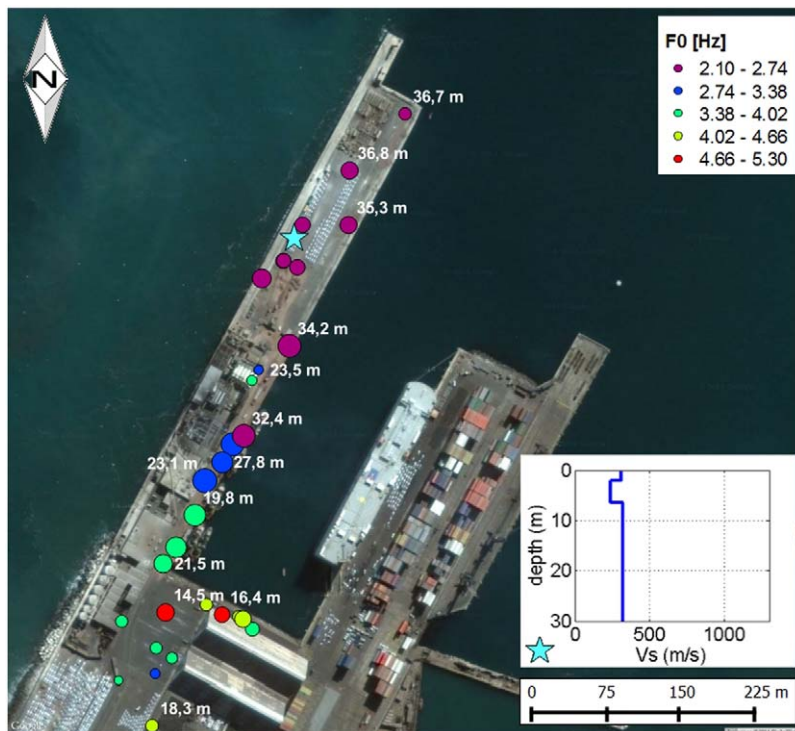


Figure 7. Geophysical characterization of the port of Iquique. The figure shows the predominant frequency of the soil and a typical shear wave velocity profiles for the pier. The white numbers indicate the estimated depth to bedrock.

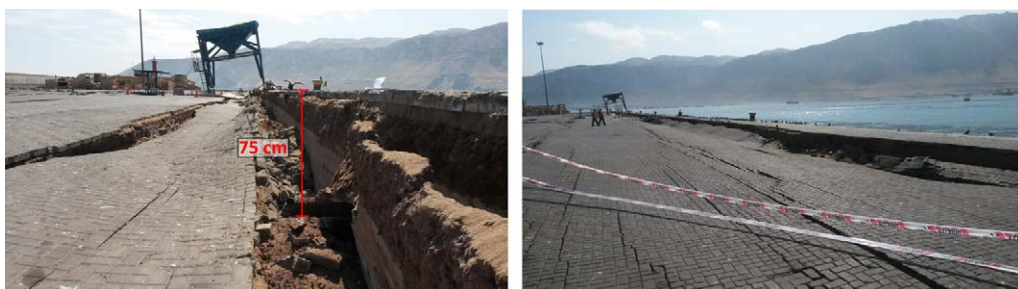


Figure 8. Observed damage in the western pier of the port of Iquique.

CASE 3: DUNAS I

“Dunas I” is a group of apartment buildings located to the east of Iquique (Figure 2). The seismic microzoning in Iquique characterizes this area as deposits of eolian sands of moderate thickness (Becerra et al. 2014). The buildings are made of confined masonry and their height

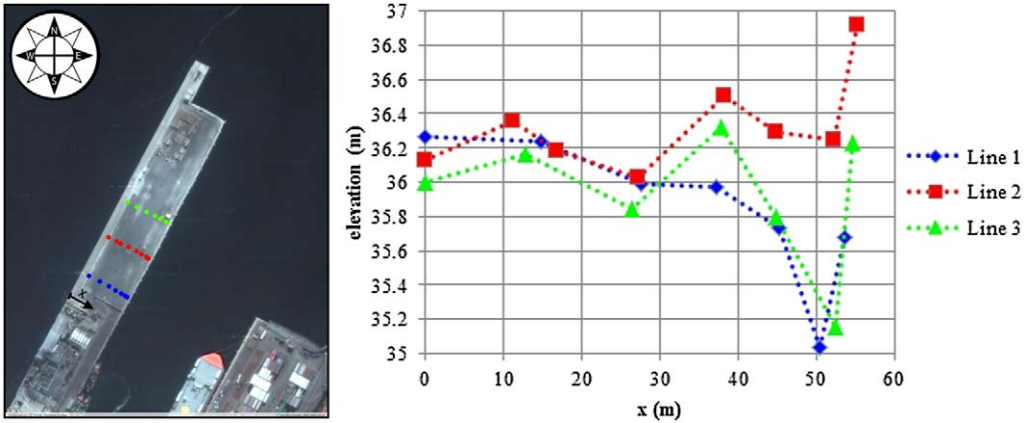


Figure 9. GPS measurements in the port of Iquique after the earthquake.

goes up to 4 stories. Based on their different plan dimensions, two types of buildings can be distinguished: type A and type B as illustrated in Figure 11. Both buildings are connected only by a central steel stairs simply supported on masonry walls. The only structural difference between them is their length; however, structural damage was seen only in the shorter buildings type A, in which we observed compressional failures in the columns of the first story and shear failures in the walls (Figure 10). We observed this level of damage in several buildings of the same type.



Figure 10. Observed damage in buildings type A in Dunas I.

A portable triaxial seismometer was placed on the top floor of each structure making it possible to estimate their post-seismic fundamental frequencies in the X and Y direction using the maximum amplitude of the Fourier spectrum technique. The fundamental frequencies are shown in Figure 11. Furthermore, HVSR was used on the sites to obtain the predominant frequency of the soil, as is depicted in the same figure. Note that, for building type A, the post-seismic fundamental frequency in the Y direction is almost identical to the predominant soil frequency obtained for the building.

Because buildings type B did not suffer any kind of structural damage, we suspect the damage of type A was controlled by a concordance of the resonant frequencies of the soil and the structure. Further studies such as synchronized recording to perform a detailed modal identification will be performed in order to confirm this hypothesis.

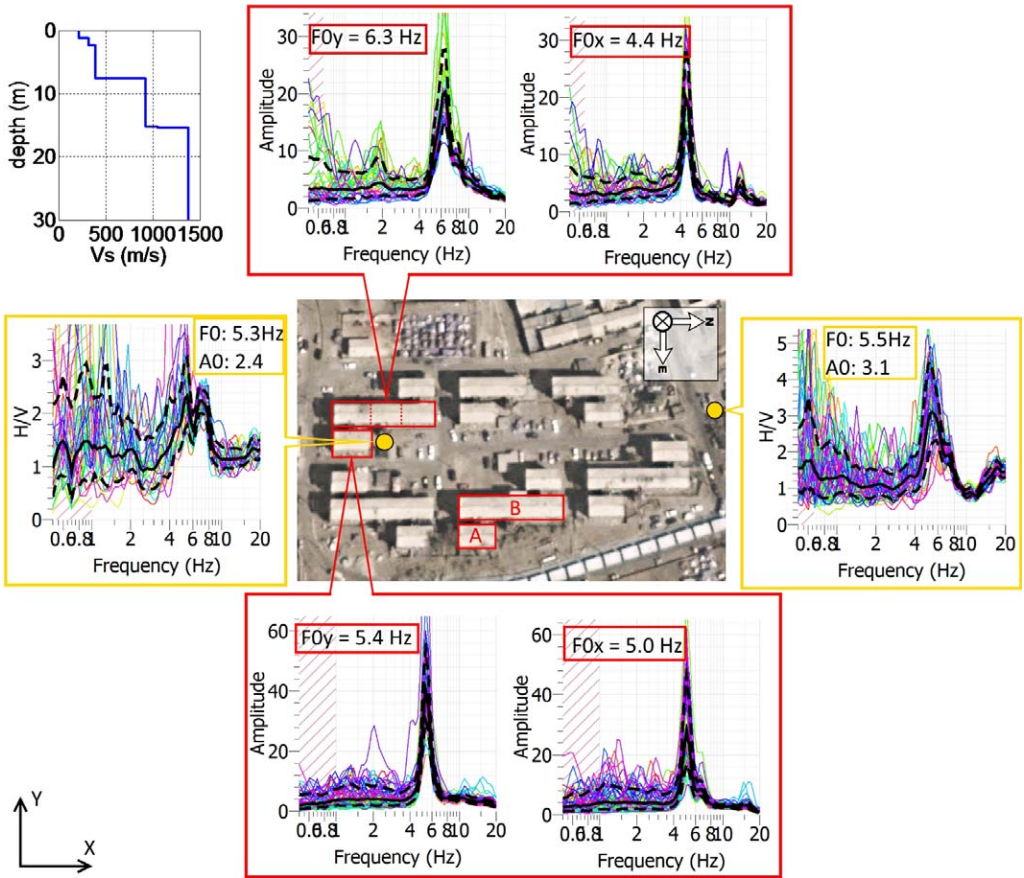


Figure 11. Types of structures (A and B) with their respective fundamental frequencies and predominant frequencies of the soil.

CASE 4: ALTO HOSPICIO

Alto Hospicio is located above the Coastal Range escarpment (Figure 2) at about 550 m above sea level. The soil beneath the city is characterized by rigid gravels with a matrix of halite (also known as rock salt) (Marquardt et al. 2008). Most of the damage in this area was concentrated in masonry houses of up to two stories near the center of the city. This is the case of Santa Eloisa condominium, shown in Figure 12, where several houses were heavily affected by the earthquake.

This area is characterized by stiff soils as is shown in Figure 13. Additionally, the strong motion record showed a slight increase compared to the one measured on stiffer soils, from 0.27 g to 0.44 g, as shown in Figure 2. Figure 13 shows the most affected house in the condominium, which shows shear wall failures all along the structure, while Figure 13 presents an example of the post-seismic cracks and cavities detected during the post-earthquake survey. This evidence suggests that partial dissolution of soil salts prior to the shaking may have generated unstable areas (cavities) that were activated during the earthquake, because near the houses, several cavities were identified on the surface, as well as seismically induced cracks on the pavement (Figure 12).

This type of soil effect cannot be associated directly with the dynamic properties of the soil measured by geophysical techniques, but it is an indirect consequence of potential instabilities of this kind of soil triggered by salts dissolution. During the campaign in Alto Hospicio, we found cavities over 5 m deep caused by the rupture of underground pipes. In order to validate this hypothesis in all the cases around the cities, radar measurements will be carried out to identify cavities that are not visible at the surface.

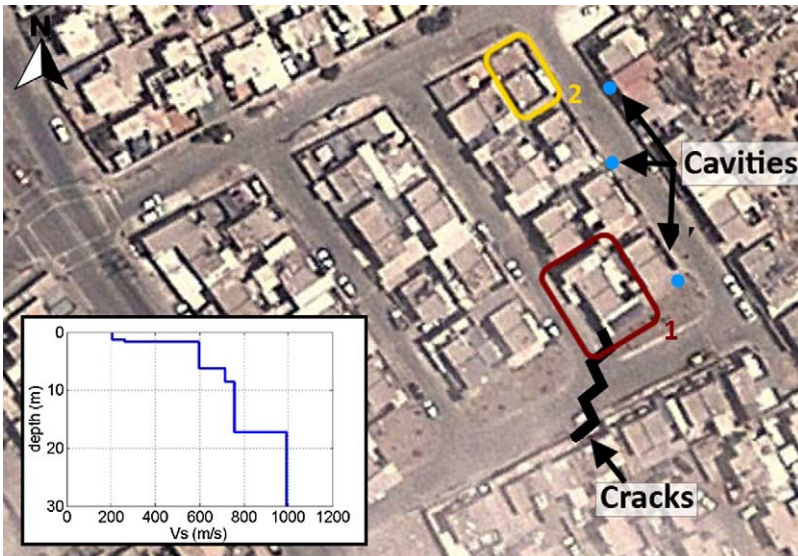


Figure 12. Map of the observed cases of interest in Santa Eloisa condominium and typical shear wave velocity profile for this area.



Figure 13. Observed damage for Houses 1 and 2. (a) House 1 shows post-seismic cracks and identified cavities, and (b) House 2 illustrates the most damaged house in Santa Eloisa condominium.

CONCLUSIONS

The 2014 Iquique earthquake occurred in an area where a grand event was expected to happen. In this context, several studies regarding the soil conditions have been performed in northern Chile. This earthquake heavily affected the cities of Iquique and Alto Hospicio.

In general, the earthquake produced significant damage in low-period structures, such as houses and warehouses, whereas most of the buildings did not show major structural problems. Indeed, the computed spectra of the earthquake showed peak periods lower than 0.2 s, which is consistent with the observed damage during the campaign. The major part of tallest buildings in Iquique (20 stories or more) are founded on rock or on cemented sand existing in the north area at a few meters deep. No significant damage was reported on these buildings.

The case studies in this paper involve some of the most significant observations from the earthquake in Iquique and Alto Hospicio. We saw that all of these cases were located in zones with rather stiff soils or artificial landfills of moderate thickness. While we can associate several causes with the observed damage, we may not disregard the effect that ground motion amplification caused on the structures.

The most affected area in the studied cities was the ZOFRI industrial zone. In this case, higher accelerations are consistent with the observed type of failure, especially in the case of the roof parapets. Although roof parapets are not structural elements, they are important due to the high risk associated with their failure.

In the port, we saw the impact of seismic design on the strength of the pier. While the seismically reinforced pier remained intact, the other one collapsed almost completely. This could have been caused for several reasons, including the low compacity of the artificial landfill and the differential height of perimeter walls around the pier.

The case of Alto Hospicio is highly interesting, as it showed the potential effects of existing cavities on saline soils under high intensity earthquakes. In this regard, we can say that geophysical data is not able to forecast the expected damage in these cases.

The Dunas I building complex is still under revision. The predominant frequency of the sedimentary soil in the area is such that a concordance of the resonant frequencies may have occurred for the shorter buildings. This case highlights the interest in evaluating the possible effects of soil-structure resonance in seismic building design.

ACKNOWLEDGMENTS

This research was funded partially by a grant from the Chilean National Commission for Scientific and Technological Research, under FONDEF+ANDES award number D10I1027 and by the National Research Center for Integrated Natural Disaster Management CONICYT/FONDAP/15110017. We would also like to thank the National Office of Emergency for contributing with the records from the 2014 Iquique earthquake and the Ministry of Housing and Urban Development for the damage report on the city of Iquique.

APPENDIX

Please refer to the online version of this paper to access the supplementary figure provided in the appendix.

REFERENCES

- Acerro, C., Augacil, G., Anastasiadis, A., and others, 2004. Guidelines for the Implementation of the H/V Spectral Ratio Technique on Ambient Vibrations Measurements, Processing and Interpretations, SESAME European Research Project, European Commission, Research General Directorate Project No. EVG1-CT-2000-00026 SESAME.
- Becerra, A., Podestá, L., Monetta, R., Sáez, E., Leyton, F., and Yañez, G., 2014. Seismic micro-zoning of Arica and Iquique, Chile, *Natural Hazards* **79**, 1–29.
- Chlieh, M., Perfettini, H., Tavera, H., Avouac, J.-P., Remy, D., Nocquet, J.-M., Rolandone, F., Bondoux, F., Gabalda, G., and Bonvalot, S., 2011. Interseismic coupling and seismic potential

- along the Central Andes subduction zone, *Journal of Geophysical Research: Solid Earth* **116**, DOI: 10.1029/2010JB008166.
- Comte, D., and Pardo, M., 1991. Reappraisal of great historical earthquakes in the northern Chile and southern Peru seismic gaps, *Natural Hazards* **4**, 23–44.
- Leyton, F., Ruiz, S., Sepúlveda, S. A., Contreras, J. P., Rebolledo, S., and Astroza, M., 2013. Microtremors' HVSR and its correlation with surface geology and damage observed after the 2010 Maule earthquake (Mw 8.8) at Talca and Curicó, Central Chile, *Engineering Geology* **161**, 26–33.
- Marquardt, C., Marinovic, N., and Muñoz, V., 2008. Geología de las Ciudades de Iquique y Alto Hospicio, Región de Tarapacá, *Carta Geológica de Chile, Serie Geología Básica* **113**, 33.

(Received 10 November 2014; accepted 27 December 2015)